PHYSICAL REVIEW E, VOLUME 63, 045305(R)

Bridge from diffusion-limited aggregation to the Saffman-Taylor problem

Vladislav A. Bogoyavlenskiy
Low Temperature Physics Department, Moscow State University, 119899 Moscow, Russia
(Received 5 July 2000; published 29 March 2001)

We introduce a Monte Carlo mean-field scheme for the diffusion-limited aggregation (DLA) model, in order to simulate processes of viscous fingering. The patterns obtained demonstrate a striking resemblance to natural shapes in Hele-Shaw cells, reproducing the Saffman-Taylor analytical solutions in the stable regime. The corresponding deterministic equations of the mean-field DLA scheme are derived and studied.

DOI: 10.1103/PhysRevE.63.045305 PACS number(s): 47.20.Hw, 47.54.+r, 61.43.Hv, 68.03.−g

Among natural nonequilibrium growth processes, the viscous fingering in Hele-Shaw cells has attracted much attention ever since the discovery of this intriguing and puzzling phenomenon [1]. It is experimentally observed that the forcing of a liquid into a more viscous one results in the complex evolution of a moving interface between the liquids, producing a wide variety of patterns—from stable smooth fingers to chaotic fractal fronts [2–5]. The relevant theoretical model is described by the Saffman-Taylor relations [6]; in the quasistationary limit the problem involves solving the Laplace equation for the pressure field $\nabla^2 p=0$ coupled with specified boundary conditions at the interface, the velocity of which, $\mathbf{v}$, is proportional to the pressure gradient ∇p.

Remarkably, the diffusion-limited aggregation (DLA) introduced by Witten and Sander as a stochastic growth algorithm [7,8] obeys the self-same hydrodynamic laws [9–12]. In this model, fractal ramified clusters grow via irreversible attachment of particles randomly walking on a lattice, so the role of the pressure field is played by the probability of visiting a lattice site. As a consequence, one may conclude that the DLA paradigm should reproduce solutions of the Saffman-Taylor problem in the mean-field limit [10–14], in agreement with the known qualitative resemblance between stable viscous fingers and an ensemble average of DLA clusters [15]. Although the connection of the models appears to be obvious, the adequate formulation of a mean-field DLA theory (i.e., the transition from discrete units to continuum walker and cluster distributions) has been a challenge for the last two decades [16–20].

Beginning from the original on-lattice DLA algorithm [7], its mean-field generalization can in principle be constructed as follows. Let us consider an integer positive number K, the discreteness parameter of the cluster distribution $\rho(\mathbf{r})$; for a lattice site, the value of ρ is an element of the finite set $\{1,(K-1)/K,(K-2)/K,\ldots,2/K,1/K,0\}$. Then the mass diffusion is modeled by the flux of walkers transferring a constant portion $u_0\equiv 1/K$ from a far source to the growing cluster. Since this scheme provides nonempty spectrum of ρ values between the extremes 0 and 1, the probability of walker aggregation $P(\mathbf{r})$ depending on the cluster field has to be defined. While a walker released from the source executes stochastic motion, at each time step a random number $R\in(0,\ldots,1)$ is generated and compared with $P(\mathbf{r})$. If $R<P(\mathbf{r})$, the walker transforms into the lattice site and advances the cluster density $\rho(\mathbf{r})$ by the value of u_0; otherwise, the wandering is continued. As successive walkers repeat the procedure, the cluster field $\rho(\mathbf{r})$ is modified. For $K=1$, this Monte Carlo scheme coincides with the regular Witten-Sander algorithm; when K goes to infinity, it describes the mean-field limit of the DLA model.

The issue of this formulation consists in the question of how to define the probability of walker aggregation $P(\mathbf{r})$ in the general case of neighboring cluster distributions. To solve the problem posed, we discuss the aggregation process in terms of the Boltzmann theory of irreversible transitions [21]. By this approach, the DLA model represents a two-particle interaction between walker $u(\mathbf{r},t)$ and cluster $\rho(\mathbf{r},t)$ fields, the intensity of which $St(\mathbf{r},t)\equiv\partial\rho(\mathbf{r},t)/\partial t$ (the Boltzmann integral of collisions) follows from the relation

$$St(\mathbf{r},t)=\int_{\mathbf{r}+\mathbf{e}\in I} u(\mathbf{r},t)\rho(\mathbf{r}+\mathbf{e},t)w(\mathbf{r},\mathbf{e},t)dI. \qquad (1)$$

Here the integration is performed inside the collision sphere $\mathbf{r}+\mathbf{e}\in I$ including all the cluster units $\rho(\mathbf{r}+\mathbf{e},t)$ neighboring the walker unit $u(\mathbf{r},t)$; the term $w(\mathbf{r},\mathbf{e},t)$ sets the probability of a successful interaction (i.e., leading to aggregation). Since the mean-field theory should satisfy the cutoff condition of growth rate at small cluster densities, we suggest the hypothesis that the interaction probability is a linear function of the neighboring cluster field. Based on this assumption, we introduce the isotropic measure for $w(\mathbf{r},\mathbf{e},t)$ as

$$w(\mathbf{r},\mathbf{e},t)=\int_{\mathbf{r}+\mathbf{e}\in I}\rho(\mathbf{r}+\mathbf{e},t)dI. \qquad (2)$$

For on-lattice processes, the integration in Eqs. (1) and (2) is transformed to a finite summation over the vector set $\mathbf{e}_i$ to adjacent sites, and one obtains

$$\frac{\partial\rho(\mathbf{r},t)}{\partial t}=u(\mathbf{r},t)\left\langle\sum_i \rho(\mathbf{r}+\mathbf{e}_i,t)\right\rangle^2. \qquad (3)$$

The last relation answers the question about the probability of walker aggregation $P(\mathbf{r})$, which is determined by the formula

$$P(\mathbf{r})=\left\langle\sum_i \rho(\mathbf{r}+\mathbf{e}_i)\right\rangle^2. \qquad (4)$$

In order to test the capability of the mean-field scheme introduced, let us consider the Saffman-Taylor configuration [6] of a long linear channel of width W. The translation invariance of the problem implies the reflection condition for wandering walkers on the lateral walls $|y|=W/2$. Here we

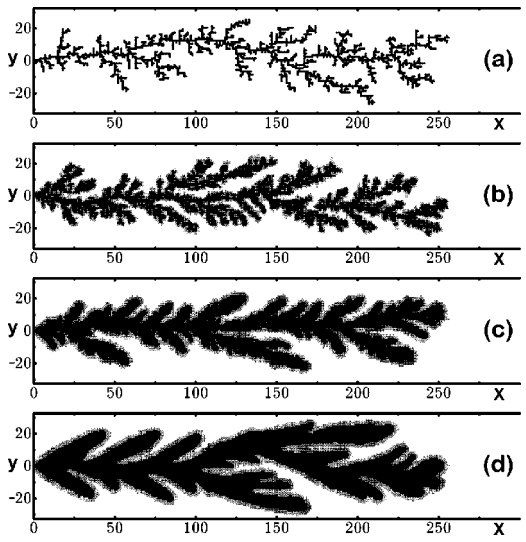

FIG. 1. Mean-field DLA simulation on a square grid (x,y) of spacing $a=1$ inside a channel of width $W=64a$. Aggregation probability $P(x,y)$ is set by Eq. (5); discreteness $K=1$, 2^4, 2^8, and 2^{12} for plots (a), (b), (c), and (d), respectively. Cluster field $\rho(x,y)$ is represented by filled ($\rho\geqslant\overline{\rho}$) or open ($\rho<\overline{\rho}$) dots, divided by the mean density $\overline{\rho}$.

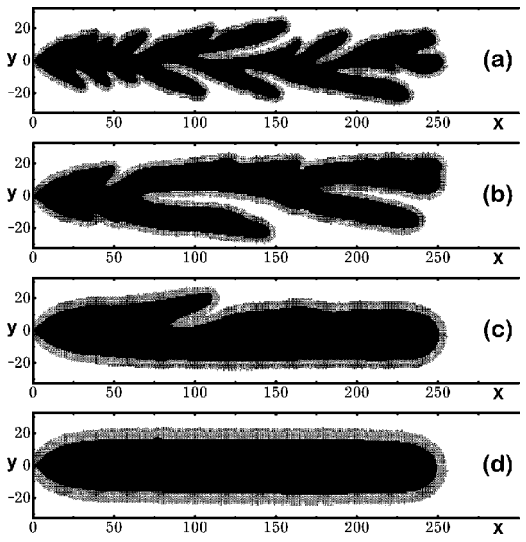

FIG. 2. Mean-field DLA simulation on a square grid (x,y) of spacing $a=1$ inside a channel of width $W=64a$. Aggregation probability $P(x,y)$ is set by Eq. (7) with $\xi=1$, 2, 3, and 3.5 for plots (a), (b), (c), and (d), respectively; discreteness is fixed, $K=2^{12}$. Cluster field $\rho(x,y)$ is represented by filled ($\rho\geqslant\overline{\rho}$) or open ($\rho<\overline{\rho}$) dots, divided by the mean density $\overline{\rho}$.

take a square grid $\mathbf{r}=(x,y)$ of spacing a and assume only nearest-neighborhood interactions, so the aggregation probability $P(x,y)$ is calculated as ($\pm$ denotes the sum of $+$ and $-$ terms)

$$P(x,y)=\langle\rho(x\pm a,y)+\rho(x,y\pm a)\rangle^2. \tag{5}$$

In Fig. 1, we summarize results of simulations inside a channel of width $W=64a$ where the discreteness parameter K is varied in the range $[1,\ldots,2^{12}]$. The case $K=1$ describes a regular DLA shape; increase of K leads to a successive thickening of cluster branches, and the last two patterns look like unstable viscous fingers observed in Hele-Shaw cells [3–5]. Thus the mean-field scheme yields a capillary length l_c to the DLA model that immediately raises the next problem—how to vary l_c, e.g., to enlarge it up to values comparable with the channel width W, to reproduce stable Saffman-Taylor fingers?

The simplest solution consists in further increase of K; this is, however, unpromising since the dependence $l_c(K)$ conjectured from our simulations is too weak, $l_c\propto\log K$, so stable patterns in the channel $W=64a$ cannot be obtained even at $K=2^{20}$. In order to find a more efficient way to increase l_c without substantial increase of computational time (which is directly proportional to K), let us discuss the length scale origin in our theory. Indeed, the sum of neighboring cluster densities in Eq. (5) represents the discrete Laplacian operator,

$$\rho(x\pm a,y)+\rho(x,y\pm a)\simeq[1+(a^2/4)\nabla^2]\rho(x,y). \tag{6}$$

By this relation, l_c originates from the term $(a^2/4)^{1/2}=a/2$, the characteristic small scale of a square grid of spacing a. Hence, a valid substitution $a^2/4\leftrightarrow\delta^2$ in Eq. (6) transforms the microscale from $a/2$ to δ; this replacement modifies the aggregation probability formula from Eq. (5) to

$$P(x,y)=\langle\rho(x\pm a,y)+\rho(x,y\pm a)-\xi\rho(x,y)\rangle^2, \tag{7}$$

where the coefficient ξ and the scale δ are related as

$$\xi=4-\frac{a^2}{\delta^2}\Leftrightarrow\delta=\frac{a}{\sqrt{4-\xi}}. \tag{8}$$

The variation of ξ in the range $[0,\ldots,4)$ allows us to enlarge the capillary length $l_c\propto\delta$ considerably, as illustrated in Fig. 2. The patterns for $1\leqslant\xi\leqslant3$ represent still unstable viscous fingers with remarkable effects of tip splitting, side branching, and wobbling, relevant to experimentally observed shapes [3–5]. When one proceeds to $\xi=3\frac{1}{2}$, the capillary length increases enough to provide stable front propagation so the cluster field takes the shape of a single Saffman-Taylor finger. For detailed investigation of the steady-state fingering, we have simulated the mean-field scheme inside a wider channel, $W=100a$, with $\xi=3\frac{3}{4}$ ($\delta=2a$); results are shown in Fig. 3. Starting from center of the channel in the beginning, first there is a region of initial transients. Then the lateral boundaries impose a time-independent shape of the propagating finger—the cluster front moves through the channel at constant velocity whereas the transverse density profile $\rho_T(y)$ approaches a step function as is required.[1] In this steady-state regime, the relative

[1]A liquid flow being modeled by the cluster field ρ naturally predetermines the following step-type conditions: $\rho=$const inside the liquid region and $\rho=0$ elsewhere.

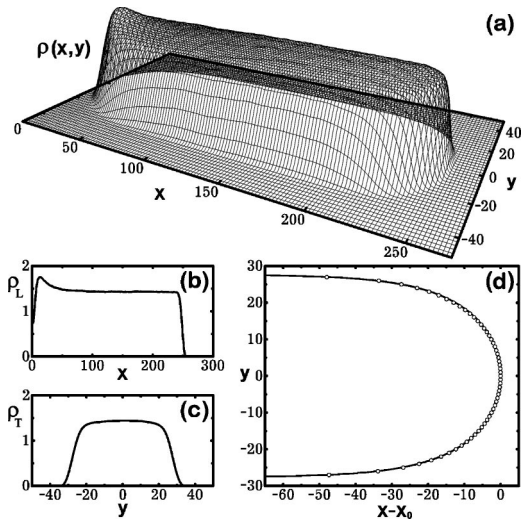

FIG. 3. Mean-field DLA simulation on a square grid (x,y) of spacing $a=1$ inside a channel of width $W=100a$. Aggregation probability $P(x,y)$ is set by Eq. (7) with $\xi=3\frac{3}{4}$ ($\delta=2a$); discreteness $K=2^{12}$. (a) Three-dimensional (3D) representation of the cluster field $\rho(x,y)$. (b) Longitudinal profile of $\rho(x,y)$ along x axis, $\rho_L(x)\equiv\rho(x,0)$. (c) Transverse profile of $\rho(x,y)$ averaged over 10 sections in the steady-state region, $\rho_T(y)\equiv(1/10)\Sigma_{x=146}^{155}\rho(x,y)$. (d) Contour plot of the mean density (open circles), $\rho(x,y)=\overline{\rho}$, compared with the Saffman-Taylor solution (continuous curve) with $\lambda=0.554$.

finger width λ measured at the mid-height of the transverse profile gives the value $\lambda=0.554$, the result of the Saffman-Taylor problem extended for the case of a finite surface tension [22–24],

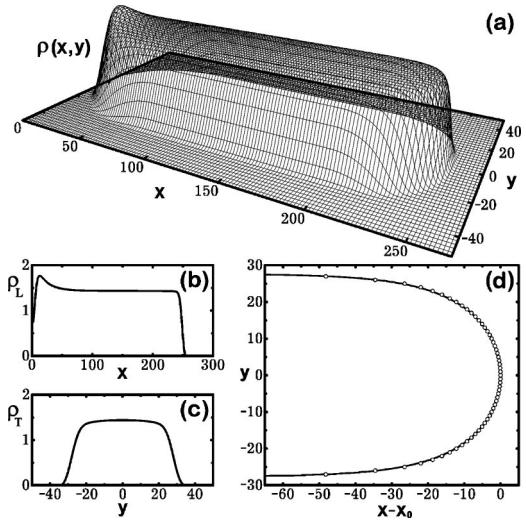

FIG. 4. Deterministic mean-field DLA model [Eqs. (11) and (12)] on a square grid (x,y) of spacing $a=1$ inside a channel of width $W=100a$; microscale $\delta=2a$. (a) 3D representation of the cluster field $\rho(x,y)$. (b) Longitudinal profile of $\rho(x,y)$ along x axis, $\rho_L(x)\equiv\rho(x,0)$. (c) Transverse profile of $\rho(x,y)$ averaged over 10 sections in the steady-state region, $\rho_T(y)\equiv(1/10)\Sigma_{x=146}^{155}\rho(x,y)$. (d) Contour plot of the mean density (open circles), $\rho(x,y)=\overline{\rho}$, compared with the Saffman-Taylor solution (continuous curve) with $\lambda=0.554$.

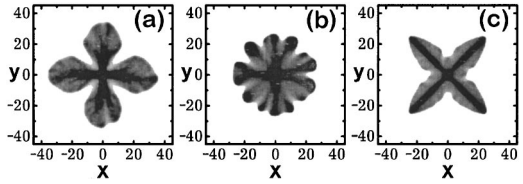

FIG. 5. Mean-field DLA simulation on a square grid (x,y) of spacing $a=1$ in the open circular geometry (the radial configuration). Aggregation probability is calculated by the following formula: $P(x,y)=\langle\rho(x\pm a,y)+\rho(x,y\pm a)\rangle^{1+\alpha}$ with $\alpha=0.5$, 1, and 1.5 for plots (a), (b), and (c), respectively; discreteness is fixed, $K=2^{16}$.

$$\lambda(l_c)=\frac{1}{2}+0.114\left(\frac{l_c}{W}\right)^{4/3}, \tag{9}$$

with $l_c\approx 57a$. At the finger tip, the contour plot of the mean cluster density precisely fits the Saffman-Taylor analytical solution [6] (x_0 is the tip position as $y=0$)

$$x(y)-x_0=\frac{W(1-\lambda)}{2\pi}\ln\left[\frac{1}{2}\left(1+\cos\frac{2\pi y}{\lambda W}\right)\right]. \tag{10}$$

Corresponding deterministic equations of the mean-field DLA model can be derived directly from the approach used to obtain the stochastic Monte Carlo scheme. Considering the limit $K\to\infty$, we proceed to continuum distributions for the cluster $\rho(\mathbf{r},t)$ and walker $u(\mathbf{r},t)$ fields. Then the expression for the cluster growth rate [Eq. (3)] is rewritten as

$$\frac{\partial\rho(\mathbf{r},t)}{\partial t}=u(\mathbf{r},t)\langle\rho(\mathbf{r},t)+\delta^2\nabla^2\rho(\mathbf{r},t)\rangle^2. \tag{11}$$

Here we substitute the Laplacian for the sum of neighboring cluster densities [Eq. (6)]; the microscale δ is introduced as a parameter of the theory. For the walker field $u(\mathbf{r},t)$, we replace the stochastic wandering by a deterministic law that accounts for the mass conservation in a diffusive system:

$$\frac{\partial\rho(\mathbf{r},t)}{\partial t}=\nabla^2 u(\mathbf{r},t), \tag{12}$$

where the growth process is considered as quasistationary, $\partial u(\mathbf{r},t)/\partial t=0$. Remarkably, these mean-field relations coincide closely with the ones originally proposed by Witten and Sander [7]; we have only changed the exponent in Eq. (11) from 1 to 2. The modification is nevertheless crucial since it provides the linear stability of the cluster front to infinitesimal perturbations. The cluster-walker interface is stable, from a theoretical point of view, for all values of δ; in practical simulations, however, Eq. (11) is extremely sensitive to numerical noise coming from unavoidable residual errors. The noise amplitude needed to drive the system unstable decreases exponentially with δ,[2] so solutions of the deter-

[2]Similar exponential sensitivity to numerical noise is observed also for the original Saffman-Taylor equations with surface tension; see, e.g., Refs. [25,26].

ministic equations are characterized by a length scale of stable behavior $l_c \propto \delta$ as are the patterns grown by the stochastic algorithm.

To compare the deterministic and stochastic mean-field DLA models, we take the Saffman-Taylor configuration of the channel of width W. On the lateral boundaries, we impose the Neuman condition for the ρ field and the Dirichlet condition for the u field, $\rho=0$ and $\partial u/\partial y=0$ as $|y|=W/2$; at infinity, we fix the flux of walkers $\partial u/\partial x=\varphi$ as $x\to\infty$ (solutions of the problem do not depend on the flux intensity φ). The numerics of Eqs. (11) and (12) is performed on a square grid of spacing a inside a channel of width $W=100a$ with $\delta=2a$; results are presented in Fig. 4. The fingerlike cluster obtained demonstrates surprisingly the same properties as the corresponding shape simulated by the stochastic scheme (Fig. 3).

In discussion, we would like to justify the hypothesis that was suggested at the beginning of our theory: ''the interaction probability $w(\mathbf{r},\mathbf{e},t)$ is a linear function of the neighboring cluster field'' [Eq. (2)]. Undoubtedly, any power-law dependence with an exponent $\alpha>0$ satisfies the cutoff condition $w\to 0$ at $\rho\to 0$ as well as the linear connection proposed, so why do we consider the special case $\alpha=1$? To clarify this question, we have simulated the relevant Monte Carlo schemes in the open circular geometry (the radial configuration) for the general case of the exponent α. As a result, all the values $\alpha>0$ provide linearly stable fronts, but the underlying lattice drastically influences the overall cluster shape by the appearance of preferential growth directions.[3] From Fig. 5, on the square grid the patterns with $\alpha<1$ are oriented along the x and y axes, whereas the choice of $\alpha>1$ leads to xy diagonal orientation; the golden mean $\alpha=1$ corresponds to circular-shaped clusters. However, the mean-field DLA theory should describe, in principle, the liquid flow as isotropic for the background, the result achieved only with the linear dependence in Eq. (2). Is this natural? We expect further theoretical clarifications of this topic.

[3]For a comprehensive analysis of reasons why cluster anisotropy systematically appears in on-lattice DLA simulations, see Refs. [27–30].

[1] H.J.S. Hele-Shaw, Nature (London) **58**, 34 (1898).
[2] D. Bensimon, L.P. Kadanoff, S. Liang, B.I. Shraiman, and C. Tang, Rev. Mod. Phys. **58**, 977 (1986).
[3] D.A. Kessler, J. Koplik, and H. Levine, Adv. Phys. **37**, 255 (1988).
[4] *Dynamics of Curved Fronts*, edited by P. Pelcé (Academic, Orlando, 1988).
[5] K.V. McCloud and J.V. Maher, Phys. Rep. **260**, 139 (1995).
[6] P.G. Saffman and G.I. Taylor, Proc. R. Soc. London, Ser. A **245**, 312 (1958); P.G. Saffman, Q. J. Mech, Q. J. Mech. Appl. Math. **12**, 146 (1959); G.I. Taylor and P.G. Saffman, *ibid.* **12**, 265 (1959).
[7] T.A. Witten and L.M. Sander, Phys. Rev. Lett. **47**, 1400 (1981); Phys. Rev. B **27**, 5686 (1983).
[8] For a review of DLA algorithms, see P. Meakin, in *Phase Transitions and Critical Phenomena*, edited by C. Domb and J.L. Lebowitz (Academic, New York, 1988), Vol. 12, p. 336; L.M. Sander, Contemp. Phys. **41**, 203 (2000), and references therein.
[9] L. Paterson, Phys. Rev. Lett. **52**, 1621 (1984).
[10] C. Tang, Phys. Rev. A **31**, 1977 (1985).
[11] L.P. Kadanoff, J. Stat. Phys. **39**, 267 (1985).
[12] Z. Koza, J. Phys. A **24**, 4895 (1991).
[13] B.K. Johnson and R.F. Sekerka, Phys. Rev. E **52**, 6404 (1995).
[14] T.C. Halsey, Phys. Today **53** (11), 36 (2000).
[15] A. Arnéodo, Y. Couder, G. Grasseau, V. Hakim, and M. Rabaud, Phys. Rev. Lett. **63**, 984 (1989); A. Arnéodo, J. Elezgaray, M. Tabard, and F. Tallet, Phys. Rev. E **53**, 6200 (1996).
[16] M. Nauenberg, Phys. Rev. B **28**, 449 (1983); M. Nauenberg, R. Richter, and L.M. Sander, *ibid.* **28**, 1649 (1983); R. Ball, M. Nauenberg, and T.A. Witten, Phys. Rev. A **29**, 2017 (1984).
[17] L.M. Sander, P. Ramanlal, and E. Ben-Jacob, Phys. Rev. A **32**, 3160 (1985).
[18] E. Brener, H. Levine, and Y. Tu, Phys. Rev. Lett. **66**, 1978 (1991); H. Levine and Y. Tu, Phys. Rev. A **45**, 1044 (1992); **45**, 1053 (1992).
[19] P. Keblinski, A. Maritan, F. Toigo, and J.R. Banavar, Phys. Rev. E **49**, R4795 (1994); P. Keblinski, A. Maritan, F. Toigo, R. Messier, and J.R. Banavar, *ibid.* **53**, 759 (1996).
[20] V.A. Bogoyavlenskiy and N.A. Chernova, Phys. Rev. E **61**, 5422 (2000).
[21] L. Boltzmann, Wien. Ber. **66**, 275 (1872) [English translation in *Kinetic Theory II*, edited by S.G. Brush (Pergamon, Oxford, 1966)].
[22] B. Shraiman, Phys. Rev. Lett. **56**, 2028 (1986); D. Bensimon, P. Pelcé, and B.I. Shraiman, J. Phys. (Paris) **48**, 2081 (1987).
[23] D.C. Hong and J. Langer, Phys. Rev. Lett. **56**, 2032 (1986); Phys. Rev. A **36**, 2325 (1987).
[24] R. Combescot, T. Dombre, V. Hakim, Y. Pomeau, and A. Pumir, Phys. Rev. Lett. **56**, 2036 (1986); Phys. Rev. A **37**, 1270 (1988).
[25] D. Bensimon, Phys. Rev. A **33**, 1302 (1986).
[26] A.J. DeGregoria and L.W. Schwartz, J. Fluid Mech. **164**, 383 (1986); Phys. Rev. Lett. **58**, 1742 (1987); L.W. Schwartz and A.J. DeGregoria, Phys. Rev. A **35**, 276 (1987).
[27] R.C. Ball and R.M. Brady, J. Phys. A **18**, L809 (1985); R.C. Ball, R.M. Brady, G. Rossi, and B.R. Thompson, Phys. Rev. Lett. **55**, 1406 (1985).
[28] P. Meakin, Phys. Rev. A **33**, 3371 (1986); P. Meakin, R.C. Ball, P. Ramanlal, and L.M. Sander, *ibid.* **35**, 5233 (1987).
[29] Y. Couder, F. Argoul, A. Arnéodo, J. Maurer, and M. Rabaud, Phys. Rev. A **42**, 3499 (1990); A. Arnéodo, F. Argoul, Y. Couder, and M. Rabaud, Phys. Rev. Lett. **66**, 2332 (1991).
[30] V.A. Bogoyavlenskiy, Phys. Rev. E **63**, 011602 (2001).